Article

JOURNAL OF COMPOSITE MATERIALS

Journal of Composite Materials
2023, Vol. 57(1) 133–145

DOI: 10.1177/00219983221139790
journals.sagepub.com/home/jcm
SAGE

Stochastic modelling of continuous glass-fibre reinforced plastics–considering material uncertainty in microscale simulations

Mathieu Vinot[1], Christian Liebold[2], Tolga Usta[2], Martin Holzapfel[1], Nathalie Toso[1] and Heinz Voggenreiter[1]

Abstract

This paper presents a probabilistic micromechanics-based approach to simulate the influence of scatter sources in composite materials as an alternative to deterministic approaches. Focus is given to the effect of microscopic and macroscopic voids, material inhomogeneity induced by manufacturing processes and stochastic fibre patterns on the mechanical properties of continuous glass-fibre reinforced polymer components. Various periodic unit cells of neat resin and embedded fibre clusters are generated with random distributions of the abovementioned scatter sources, while the voids are represented by degrading locally the pristine properties in an element-wise manner. Subsequently, the models are mechanically loaded under transverse tension as an exemplary case and the resulting responses are correlated with the stochastic inputs. In particular, the relative influence of pore size, porosity and fibre/resin interface strength on the transverse tension modulus and strength of unidirectional composites are numerically investigated. The present approach is suggested as a computational efficient but reliable alternative to geometrical representations of imperfection in composite materials.

Keywords

Finite Element Analysis, composites, epoxy, micromechanics, stochastic, voids, failure

Introduction

Composite materials have increasingly replaced metallic structures in many industrial applications due to their high mass-specific mechanical properties and the weight reduction possibilities they offer. In the field of transportation systems, they are used in structures sustaining crash or impact loading because of their good energy absorption capability under certain loading conditions.[1]

However, the mechanical behaviour of composite materials is inherently influenced by multiple sources of scatter which result from the raw materials and the manufacturing processes (draping, forming, infiltration), and may hardly be described in a deterministic way. Additionally, the load spectrum during the service life can neither be assumed to be deterministic and may strongly vary depending on operative conditions. While the stochasticity is not mostly critical for the structural stiffness, its influence grows when considering structural failure and even more fatigue. The application of high safety margin in the sizing of composite structures has been widely accepted in industrial applications to cover the abovementioned uncertainties, thus reducing the lightweight efficiency of composite materials.[2,3]

Through the rapid development of computing power, multiscale simulation solutions have thrived to achieve a higher comprehension of the failure mechanisms in composite materials at different material scales.[4] Due to their deterministic nature, these numerical approaches have however lacked the necessary reliability to be fully used in the sizing of structures as an alternative to costly experimental tests. In the recent years, a paradigm shift has been

[1]German Aerospace Center (DLR), Institute of Structures and Design, Stuttgart, Germany
[2]DYNAmore GmbH, Stuttgart, Germany

Corresponding author:
Mathieu Vinot, German Aerospace Center (DLR), Institute of Structures and Design, Pfaffenwaldring 38-40, Stuttgart 70569, Germany.
Email: mathieu.vinot@dlr.de

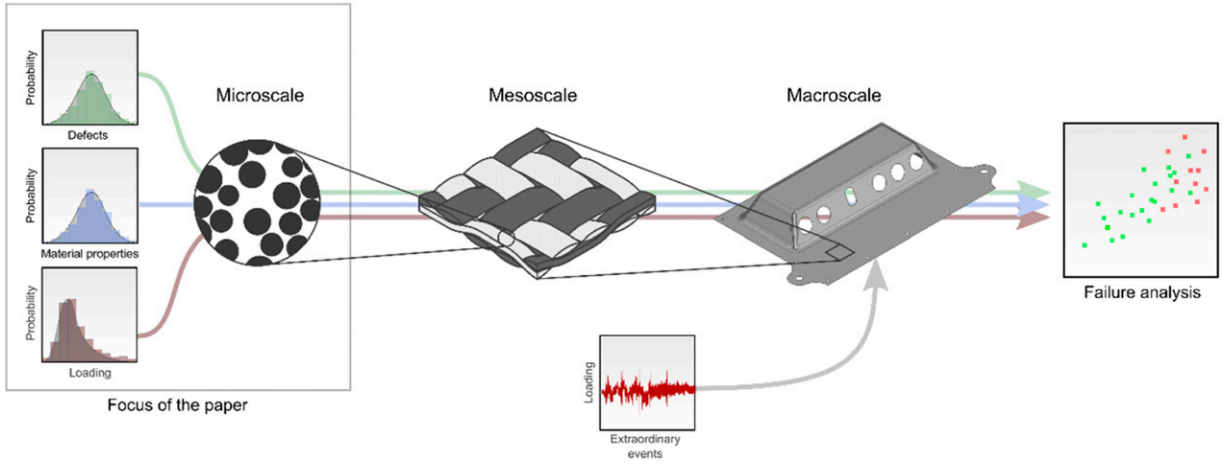

Figure 1. Representation of the multiscale framework with propagation of uncertainty effects between the material scales.

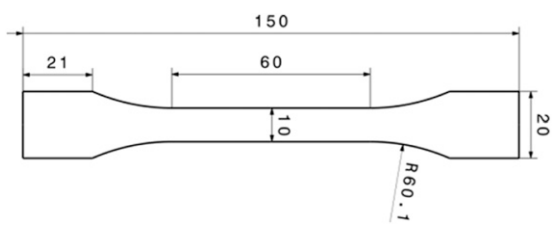

Figure 2. Specimen geometry for neat resin tension specimens.

observed from deterministic to probabilistic approaches and various research activities started to include sources of uncertainty in the simulation of composite structures.[5,6] Probabilistic simulations mainly benefit from the possibility to vary and investigate material properties or material states which sometimes cannot be measured without high experimental effort or be dependent on the manufacturing conditions and therefore vary from structure to structure.

Recent works contributed to the development of stochastic multiscale solutions using different approaches to investigate several scatter sources in composite materials. He[7] developed an approach based on the geometrical representation of sub-ply voids in unidirectional unit cells and predicted the loading-dependent drop of the material strength at increasing void contents. Using similar modelling techniques, Chu,[8] Hyde[9] and Turteltaub[10] simulated the detrimental effect of void content and void shape on the material's stiffness, strength and energy release rates respectively. The modelling of the voids has been differently handled by Liu in,[11] where elements were randomly deleted at the beginning of simulation. The authors investigated the decrease of the compression strength in various textile composites for various void contents. The modelling technique reproduced the stress concentration in the compressed yarns with higher orientation angle accurately. Liu applied the methodology to establish the influence of voids on the residual stresses resulting from hygroscopic expansion in water absorption process.[12] The chosen geometrical representation of voids increases the simulation's accuracy but inherently involves finer mesh sizes, especially in the vicinity of the microscopic voids. Consequently, higher computational efforts are necessary for the uncertainty quantification (UQ).

Composite materials are particularly sensitive on fibre-resin debonding, which lowers strongly the transverse strength of the material and plays a large role in the crack propagation mechanisms. Melro implemented a microscopic modelling approach where crack opening and propagation between the fibres and the resin material is simulated via cohesive elements.[13] With this approach, Melro predicted a strong reduction of the transverse and shear strengths of unidirectional plies.

The above-mentioned works, depicted the importance of the resin material and its properties on the behaviour of unidirectional composite plies. Another part of literature works focused on quantifying the influence of fibre repartition, shape and properties on the composite's behaviour. Swolfs contributed to the experimental characterisation of the Weibull distribution of the fibre strength with large number of samples.[14] With help of large-scale microscopic models, he outlined the importance of using random fibre packing and observed higher stress concentrations in the vicinity of broken fibres in this type of model compared to hexagonal packing. Adding to these results, AhmadvashAghbash considered additionally interface debonding in his microscale model to characterize the stress concentration factor near broken fibres.[15] The stress concentration was found to depend on various parameters, such as local fibre volume fraction (and so minimal fibre distance), interface debonding or friction.

Zheng et al.[16] proposed an algorithm bridging the microscopic and mesoscopic scales to predict the compression behaviour of 3D woven composites. The authors introduced

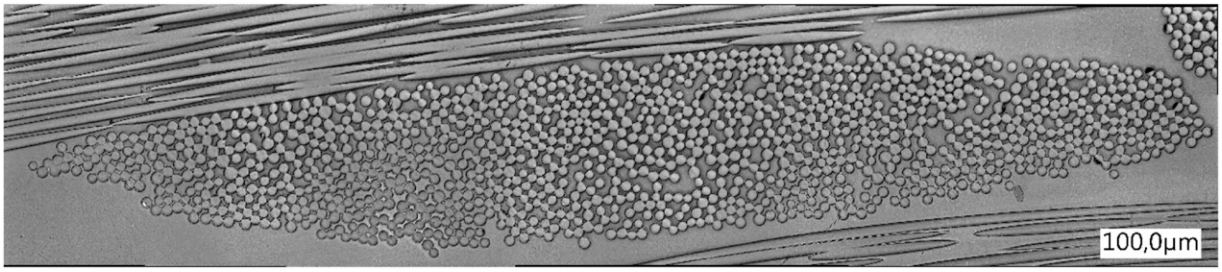

Figure 3. Reconstructed yarn from micrograph samples.

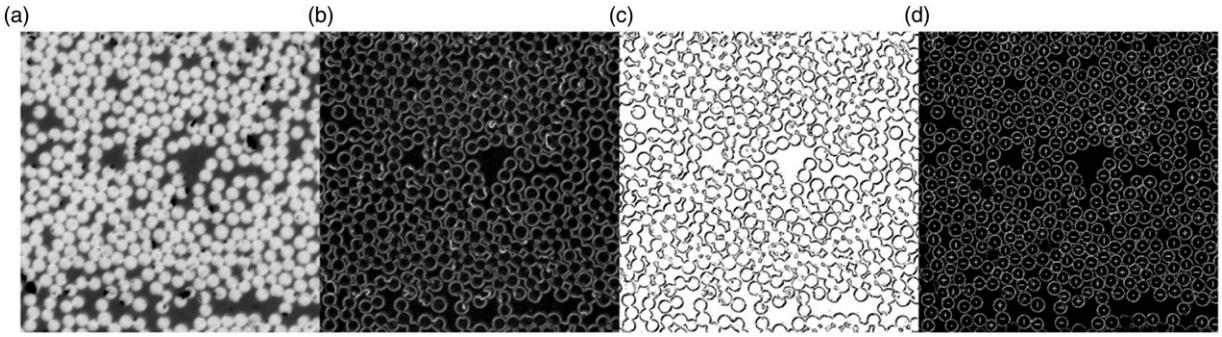

Figure 4. Automatic detection of the fibre distribution in polished micrographs with Hough Cycle Transformation.

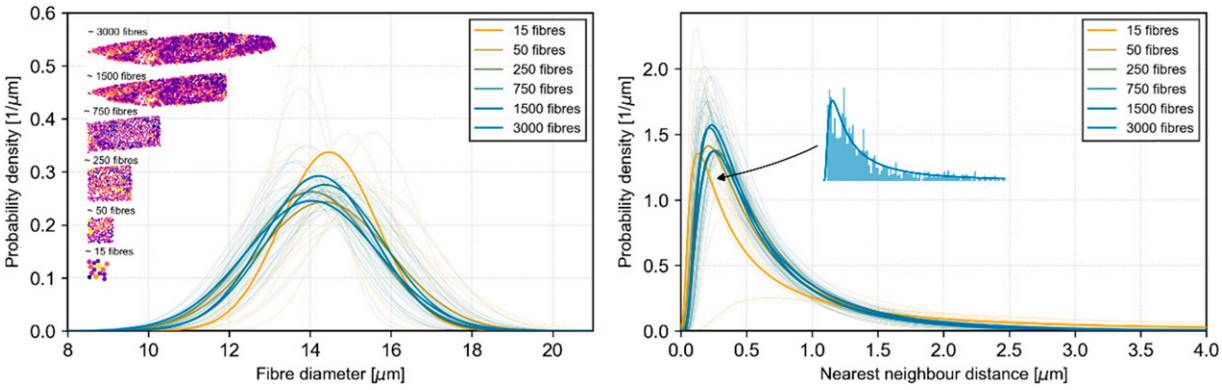

Figure 5. Plots of the average probability density curves for different subregion sizes: Probability density versus fibre diameter (left) and probability density versus nearest neighbour distance (right). Greyed curves represent the nominal distributions in single regions.

stochastic fibre misalignment and normally distributed fibre strengths in mesoscale models to simulate the kinking failure of the material under compression loading.[17] The study stressed out the strong negative effect of fibre misalignment on the compression strength, with a drop up to 40% for a 5° misalignment. Mehdikani propagated the uncertainties from microscopic models on the mesoscopic model of a multilayered laminate to study the matrix cracking mechanisms.[18] To achieve uncertainty propagation (UP), the stiffness and strength values from micromodels were attributed to "*voidy elements*" with a fixed void content. Going further, a complete UQ and propagation approach has been proposed by Bostanabad in Ref. 19 which relied on random fields to model the sources of uncertainty at the different material scales, such as fibre misalignment or fibre volume content. The approach contributed to the reduction of the computational effort for multiscale simulation by use of metamodels and by reducing the problem to the uncertainties with the highest influence on the material response. The UQ and UP scheme has been applicated to compute the linear behaviour of a woven composite under the influence of various uncertainty

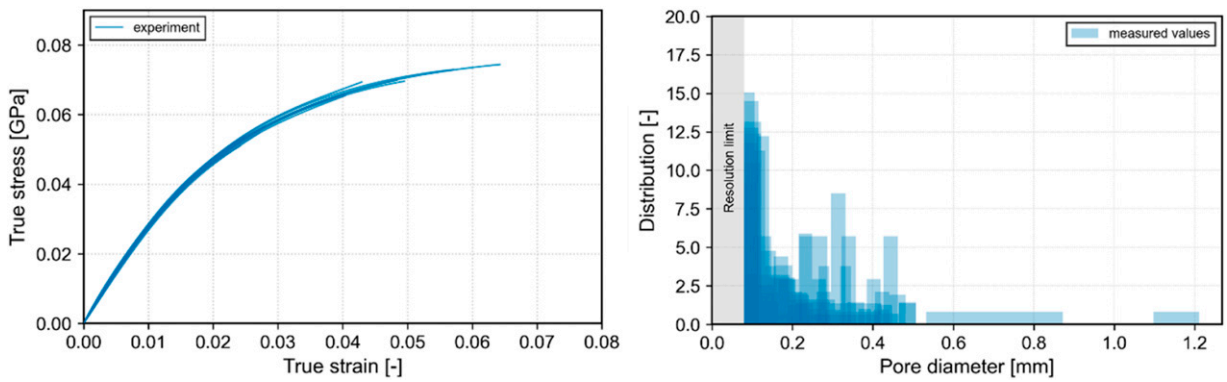

Figure 6. Measured stress–strain curves (left) and pore size distribution (right).

Table 1. Hill's anisotropic constants.

	F	G	H	L	M	N
Resin	0.5	0.5	0.5	1.5	1.5	1.5
Fibre	0.04	0.04	−0.04	0	0	0

Table 2. Mechanical properties of fibre and resin materials.

	E_{11} (GPa)	E_{22} (GPa)	E_{33} (GPa)	G_{12} (GPa)	ν_{12}
Resin	2.89	2.89	2.89	1.13	0.28
Fibre	80	80	80	33	0.22

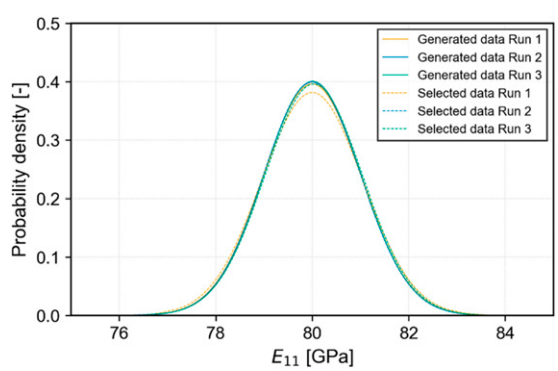

Figure 7. Gaussian distribution at the example of the axial modulus for the probabilistic simulation.

sources. The authors emphasized the required computational efficiency for the performing of multiscale simulations and for the efficient coupling between the different scales. Similar requirements have been raised by Chiachio in Ref. 20.

This paper describes the development of a numerical finite-element framework on the microscopic scale to quantify uncertainties in continuous unidirectional composites and evaluate their influence on the mechanical properties of the material. In particular, it uses a non-geometrical approach for the representation of porous regions which reduces the modelling and computing effort compared to the above-mentioned geometrical approaches. The approach attributes as well spatially varying mechanical properties described by independent Gaussian distributions on an integration-point basis. Since no mesh modification is necessary, the principle can be easily scaled up to the investigation of a larger panel of uncertainties and is equally applicable to shell elements models on the macroscale. Further sources of uncertainty such as fibre debonding are considered as well through the use of a mesh-free cohesive contact algorithm. The coupling of many uncertainty sources within the same finite-element models allows for a precise investigation of their interaction and of the degree of influence they have on the composite's mechanical properties. The extraction of metamodels, linking uncertainties to the resulting mechanical properties, via a Monte-Carlo analysis allows for an efficient transfer of the relationships on higher material scales, which is out of the focus of the present contribution. The approach finally simulates the non-linear behaviour of the composite material and its constituents, and depicts various failure modes driven by matrix plasticity, interface failure or fibre failure.

In section 2, an experimental test campaign is performed to quantify the scatter in the properties of the principal constituents of a composite material: resin material and infiltrated yarns. A numerical method is then developed in section 3 to generate and simulate stochastic representative unit cells of unidirectional composites on the microscopic scale. Finally, an investigation of the sources of uncertainty and their respective influence is performed with help of a Monte-Carlo analysis in section 4. The present work represents the first building block of a larger multiscale framework for the probabilistic investigation of composite structures, as shown in Figure 1.

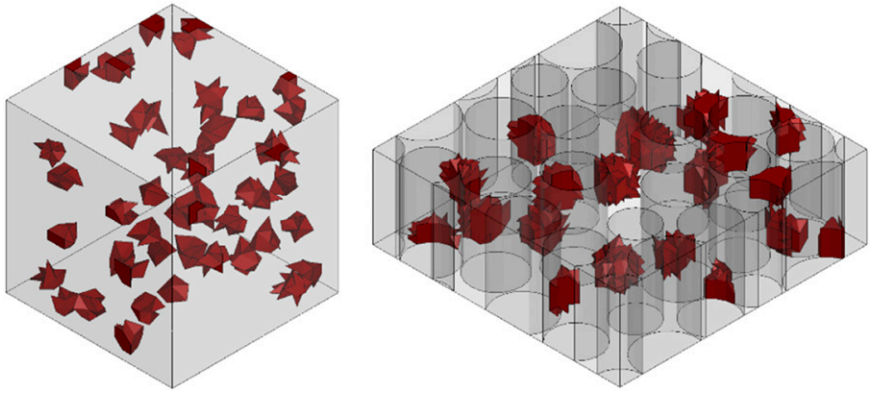

Figure 8. Generated models of a neat resin (left) and of a microscopic unit cell (right) with pores.

Experimental determination of material scatter

The development of the microscale simulation methods requires the understanding and quantification of the sources of scatter in the composite material. First, the sources of uncertainty are clustered in three categories depending on their nature. Geometric uncertainties result from the manufacturing processes and mainly concern the spatial distribution of the fibres. During the draping and the subsequent infiltration steps, the rearranging of the fibres leads to the formation of various fibre-dense clusters, resin pockets, or more generally of domains with random local fibre volume content. Moreover, local misalignment of the fibres can be observed which may strongly influence the axial mechanical properties of the compound. Constituent material property related uncertainty can mostly be affected by the resin material (heterogeneous mixing of the resin components over the part) or the properties of the interface between the resin material and the fibres. Finally, morphological uncertainty results from induced defects during the production processes, which may locally influence load paths (pores in the resin material, cracks in the composite). In the following, the above listed scatter sources will be experimentally characterised for a woven glass-fibre reinforced epoxy material as basis for the probabilistic simulation framework. In section 2.1, the considered material and the manufacturing of the specimens is presented. Section 2.2 focuses on optical measurements of the fibre distribution in the composite. In section 2.3, the neat resin is experimentally investigated.

Material system, manufacturing and test specimens

The experimental work focuses on a woven composite constituted of Johns Manville StarRov® 086 3k glass-fibre tows embedded in a high temperature epoxy resin Sika Biresin® CR170 combined to a hardener Biresin® CH170-3 at a weight mixing ratio of 100 to 16. Both neat resin plates and reinforced woven plates are first infiltrated using the RTM technique and post-cured at 160°C during 5 hours with a heating ramp of 0.2°C/min and cooling rate of 0.5°C/min up to room temperature. Specimens are finally milled out of the plates to avoid edge perturbation characteristic of other cutting methods like water jet or laser jet. For the experimental characterisation of the epoxy resin, specimens are chosen according to DIN EN ISO 527-2B[21] norm for tensile specimens (Figure 2).

Finally, polished specimens are prepared out of the infiltrated composites plates on samples with a diameter of 15 mm for further optical investigation. The specimens are first grinded with grinding plates of 60 µm and progressively polished using diamond particles of 14 µm, 9 µm, 3 µm and 0.5 µm. Between each step, the specimens are cleaned of remaining particles in an ultrasonic bath filled with osmosis water.

Investigation on polished micrographs

The polished specimens are investigated with a Keyence VHX-5000 digital microscope for measurement of the fibre dimensions and spatial distribution. The complete yarns are captured in multiple steps at a magnification factor of 1000× and reconstructed into one single image (Figure 3). The micrograph pictures are then postprocessed with the open-source software ImageJ 1.52.[22] After removing unnecessary information by adjusting the grey-value threshold (Figure 4(a)), an edge recognition step is performed (Figure 4(b)) and the processing is completed with a Hough Cycle Transformation on the inverted picture (Figure 4(c) and (d)).[23] The extracted information (position of the fibre centre point and diameter) are stored in separate files for statistical analysis.

The characteristics of the fibre clusters are represented by two statistical functions. The distribution of the fibre

Table 3. Range for the investigated parameters.

Parameter	*Min. value*	*Max. value*
Porosity	0%	5%
Macroscopic pore size	0.1 mm	2 mm
Microscopic pore size	2 μm	10 μm
Interface strength	0.020 GPa	0.150 GPa

diameter D follows the normal (or Gaussian) distribution in equation (1), in which σ and μ are the mean value and standard deviation of the data sample. This distribution has been widely used in various algorithms for the generation of microscopic models and is a realistic statistical representation of the variations in the fibre's diameter.[24,25] The second characteristic parameter is the Nearest Neighbour Distance (NND) which describes the smallest distance between one reference fibre and its neighbours. As the NND is per definition larger or equal to zero, the Gaussian distribution is replaced by the inverse normal distribution (also known as Wald distribution) which is characterised by the location parameter θ, the scale parameter λ and the mean μ (equation (2)).[26] This type of distribution depicts accurately the NND, as shown in Figure 5 for one exemplary sample of 3000 fibres. The measured NND distribution shows similar characteristics to the probability function documented in Ref. 25 for carbon fibres, with an average at about 0.5 μm

$$D(x) = \frac{1}{\sigma\sqrt{2\pi}} e^{-\frac{1}{2}\left(\frac{x-\mu}{\sigma}\right)^2} \tag{1}$$

$$NND(x) = \left(\frac{\lambda}{2\pi(x-\theta)^3}\right)^{\frac{1}{2}} e^{\left(-\frac{\lambda(x-\mu)^2}{2\theta^2(x-\theta)}\right)} \tag{2}$$

The spatial distribution of the fibres in consolidated composites is per nature stochastic and varies over the whole yarn or over the different yarns. Since finite-element simulations on the mesoscopic or macroscopic scales consider homogenised materials with a specific discretization size, it is necessary to investigate the scatter in the fibre distribution depending on the size of the postprocessed domain. To this purpose, the yarns are subdivided into rectangular regions which contains from 15 up to 3000 single fibres and the distributions for fibre diameter and NND are characterized for each region (Figure 5). In this application, the calculation of the diameter distribution is possible at every scale, while the NND should be studied at least on more than 50 fibres to diminish the influence of local effects. No voids have been detected in the investigated micrograph samples.

Material characterization of the resin BR170

In composite materials, resin material acts as stabilising system for the fibres and as load transfer medium between the fibres. Consequently, the material properties of the resin strongly influence the composite mechanical properties, particularly under transverse loading, shearing, or under axial compression, where stability issues can occur. Furthermore, strong dependencies on the resin system have been observed in literature for the energy absorption capability of composite materials in crash or impact events.[27–29] In regard to this influence, a characterization of the resin material appears mandatory in all multiscale frameworks in order to achieve a good prediction accuracy. Several literature sources observed up to 30% increase of the in-situ hardness and elastic modulus of the resin material when measured in the infiltrated composite material with nanoindentation tests compared to neat resin properties measured on bulk specimens.[30–32] Furthermore, the elastic modulus was found to be impacted by the vicinity of fibres in the indented resin pocket. The nanoindentation technique is sensitive to manufacturing conditions and to the state of the composite at the testing time. In his work, Chevalier cited amongst others the potential influence of resulting thermal stresses after curing or of material aging on the measured properties.[31] The non-destructive characterization through nanoindentation is particularly promising for the individual assessment of composite parts' performances subsequent to their manufacturing. In the present work, material characterization is performed using mechanical test procedures from norms on bulk specimens. This choice is driven by the possibility to feed the resin's material card without inverse modelling techniques. Furthermore, the resulting data and stress versus strain relationships can be easily compared to other studies working with similar methods.[33]

Under transverse tension, modelling the epoxy resin as an isotropic, elasto-plastic material with tension-compression asymmetry has yielded good predictions of the composite's behaviour in precedent literature works.[34,35] For this reason, experimental investigations will first be performed on tension specimens only. An improvement of the numerical model can be achieved by additionally investigating the compression and shear loadings and using extended failure models based for instance on the Drucker-Prager yield criterion. Twenty tension specimens from two different material plates are quasi-statically tested in a universal testing machine Zwick1494 at a crosshead speed of 2 mm/min according to the norm DIN EN ISO 527-1.[36] The tests are monitored using one camera from the LIMESS Messtechnik u. Software GmbH[37] and two-dimensional strain fields are subsequently extracted using Digital Image Correlation and virtual extensometers. Stress calculation is

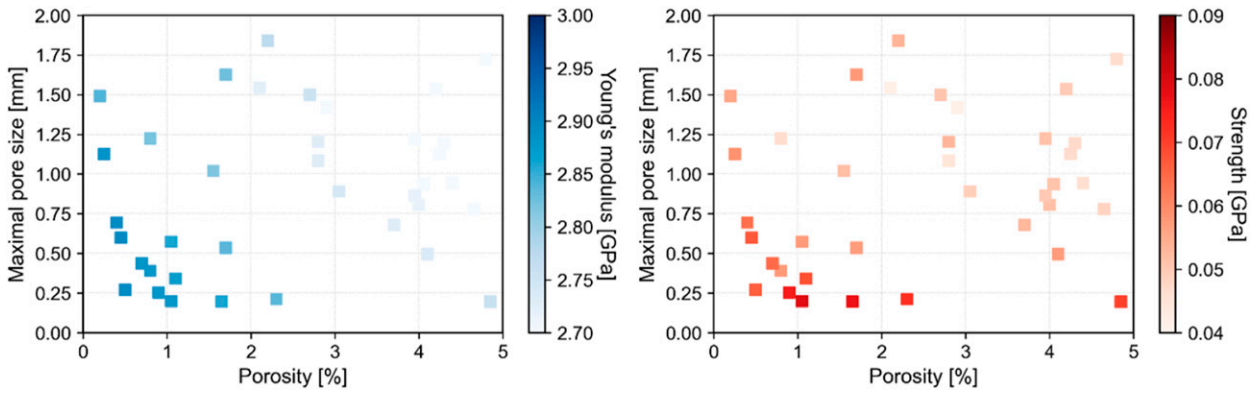

Figure 9. Relationship between porosity, pore size and material properties for neat resin.

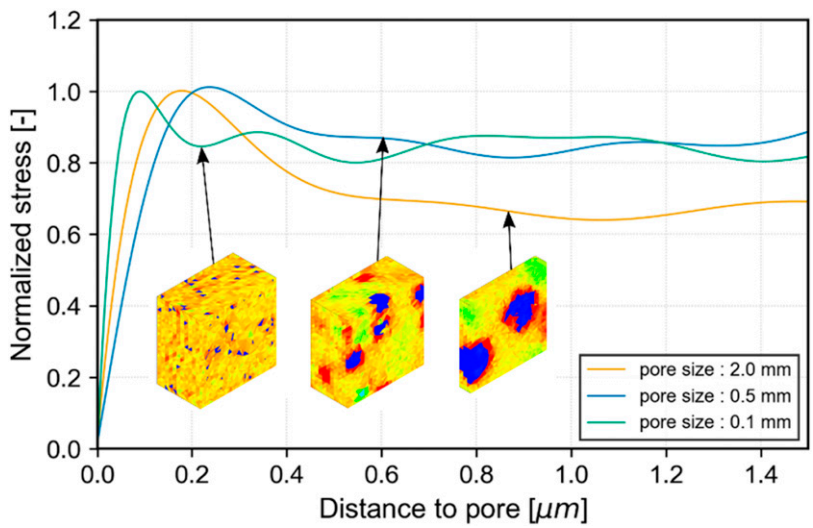

Figure 10. Stress concentration caused by the presence of pores in the neat resin.

achieved using the measured force while considering cross-section changes of the specimen throughout the test. Before testing, the resin specimens are photographed, and the pictures are treated to estimate the pore's size and density. For this, the automatic edge detection and pattern recognition features of ImageJ are used. The specimens show relatively constant pore size distributions (Figure 6, right) with a maximal pore size of about 1.2 mm. Due to the postprocessing methodology used, pores below 0.1 mm diameter could not be detected. The unidirectional composite material could not be tested experimentally and will only be numerically investigated in section 4. Both the measured Young's modulus and the measured material strength follow a normal distribution with mean values of 3 GPa and 0.058 GPa respectively and with standard deviations of 0.13 GPa and 0.011 GPa respectively.

Modelling of composite materials at the microscale

The experimental investigation of composite materials for certification purposes is a cost and resource-intensive task and requires a high level of repetition to capture stochastic effects. In the present section, a microscopic approach is presented to virtually investigate randomly distributed variations in resin and unidirectional composites. The model generation, material models, and algorithms used are documented.

Generation of randomly distributed unit cells

The concept of unit cell is widely employed in multiscale simulations to reduce the computation time.[38,39] Particularly, several works have developed algorithms to generate

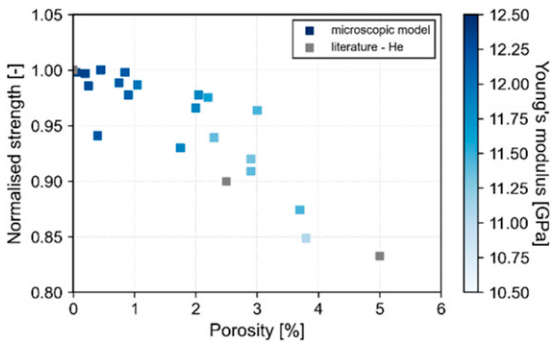

Figure 11. Predicted relationship between porosity and mechanical properties at the microscopic scale compared to the simulated value in Ref. 7.

unit cells of random fibre patterns at the microscopic scale while guarantying compatibility with periodic boundary conditions.[13,40] In the present work, 75 × 75 × 7 μm³ microscopic unit cells were created using the modified Nearest Neighbour Algorithm developed by Wang to achieve high fibre volume content of up to 70%[40] The distributions experimentally measured in section 2.2 were used for the model generation. A unit cell size of 10 times the mean fibre radius was chosen to limit the computation time as documented in Refs. 41 and 42. The unit cells consist of 2 μm tetrahedron elements with shear locking correction. 3D periodic boundary conditions are applied using the algorithm proposed by Chao in Ref. 43. Linear constraint equations are applied to corresponding nodes on external faces of the unit cell. The loading of the unit cell is defined through an imposed displacement boundary condition.

Additionally, 5 × 5 × 5 mm³ unit cells of neat resin are generated with 0.25 mm large tetrahedrons to separately investigate the effect of macroscopic pores and stochastic material properties on the neat resin behaviour. The finite-element models with 35,646 and 126,324° of freedom in total for the neat resin model and the microscopic model respectively are simulated using the explicit solver LS-DYNA R12.1 using four Intel® Core™ i7-10850H 2.70 GHz with a timestep of 1.0 × 10^{-5} ms. The neat resin model and the microscopic model computes within 1221 s and 5101 s respectively.

Material model

The present work focuses on the influence of randomly distributed defects and locally varying material properties in composite materials. To this purpose, both resin and fibre materials are modelled with an anisotropic elasto-plastic model with brittle orthotropic failure (MAT_157_ANISOTROPIC_ELASTIC_PLASTIC in LS-DYNA).[44] The material properties consisting in the ij^{th} terms of the 6 × 6 anisotropic constitutive matrix, as described in equation (3), and consisting in the strengths in 3D space are attributed in an element-wise manner for solid elements or to each integration points of shell elements at the beginning of the simulation. The resin plasticity is described by the experimentally measured stress versus strain curve with the highest strength, see Figure 6 in section 2.3, assumed to correspond to a specimen with no or neglectable defects. The resin and fibre failure follow the Tsai-Hill failure criterion from equation (4) with the Hill's parameters given in Table 1. Fibre failure is assumed to occur only in the axial direction. The stochastic distribution of the fibre axial strength, investigated by Swolfs et al. in Ref. 14, has been accounted for by using the tool described in section 0 using the suggested Weibull distribution. Other failure mechanisms in the fibres are neglected and the corresponding strengths set to an infinite value. The mechanical properties of fibre and resin materials are documented in Table 2.

Calculation of the compliance matrix

$$C^{-1} = \begin{bmatrix} \frac{1}{E_{11}} & -\frac{\nu_{21}}{E_{22}} & -\frac{\nu_{31}}{E_{33}} & 0 & 0 & 0 \\ -\frac{\nu_{12}}{E_{11}} & \frac{1}{E_{22}} & -\frac{\nu_{32}}{E_{33}} & 0 & 0 & 0 \\ -\frac{\nu_{13}}{E_{11}} & -\frac{\nu_{23}}{E_{22}} & \frac{1}{E_{33}} & 0 & 0 & 0 \\ 0 & 0 & 0 & \frac{1}{G_{12}} & 0 & 0 \\ 0 & 0 & 0 & 0 & \frac{1}{G_{23}} & 0 \\ 0 & 0 & 0 & 0 & 0 & \frac{1}{G_{31}} \end{bmatrix} \quad (3)$$

Tsai-Hill failure criterion for the fibre and the matrix materials.

$$(G+H)\sigma_{11}^2 + (F+H)\sigma_{22}^2 + (F+G)\sigma_{33}^2 - 2H\sigma_{11}\sigma_{22} - 2F\sigma_{22}\sigma_{33} - 2G\sigma_{33}\sigma_{11} + 2N\sigma_{12}^2 + 2L\sigma_{23}^2 + 2M\sigma_{31}^2 < 1 \quad (4)$$

Consideration of material uncertainty

Material uncertainty is introduced to the structure early in the manufacturing phase. Since the manufacturing process is accepted as a stochastic process by nature, determination of the level of the uncertainty is a challenging task. Locally varying material properties and non-continuous boundaries in a domain of interest, such as pores or inclusions, are two main sources of material uncertainty. Of course, the manufacturing process can be optimized to reduce uncertainty, but complete prevention

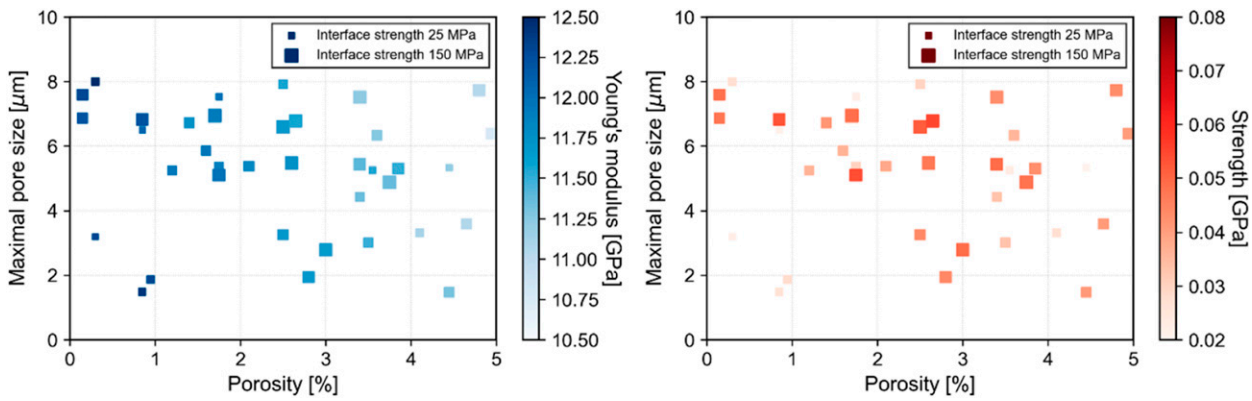

Figure 12. Relationship between porosity, pore size and material properties for neat resin; the size of the scatter points indicates the interface strength.

is not possible. Therefore, the present work uses the commercial software envyo®[45] to imitate the material uncertainty by generating randomly distributed pores (or inclusions) and modifying the material properties of fibres and resin materials using Gaussian distribution on integration point level of a unit cell finite element (FE) mesh.

The software uses real-time seeded Gaussian distribution embedded randomized algorithm according to the user defined control file. The control file consists of nominal values and standard deviations of the material parameters as well as porosity options such as minimum and maximum pore size, maximum porosity, and pore effect constant. If the pore effect constant is defined greater than 1.0, the algorithm can mimic inclusion effects by amplifying the material properties (in the scope of this work, only the pore effects are studied). Thereby the material uncertainty of a unit cell can be represented by modifying material constants and establishing a porous domain of interest.

According to the user-defined data, the software initializes material properties of each integration point randomly and generates pores using only randomly selected resin elements by degrading their stiffnesses by a factor d (standardly set as 0.01) according to the scheme described in equation (5). To avoid element deletion at higher strains, the material strengths of porous elements are set to high values.

Degraded material properties of porous elements

$$\begin{cases} C_{ij,\ pore} = C_{ij,\ 0} \cdot d \\ \sigma_{ij,\ pore} = \infty \end{cases} \tag{5}$$

Each pore generation process may be similar, but it is unique for each run for the same control file and unit cell input. The repeatability of the data set generation using Gaussian distribution is ensured (Figure 7). However, the selection of values from the generated data set is totally random. Therefore, the resulting material behaviour may be close to data set extremums. This stochastic approach provides rapid virtual data generation and robust virtual statistical investigations of the target material. The present representation of the pores by lowering the material properties locally is particularly suitable for use in fast computational models. It represents an alternative to modelling approaches as exemplary investigated in Ref. 7, which represent accurately the spherical shape of voids with finer mesh sizes. Furthermore, the present approach allows a large flexibility in the representation of multiple material phases within the same model such as the contamination with foreign particles. On the downside, the random pore generation is strongly dependent on the mesh size and on the formulation of the elements used.

Section 4 places the focus on the effect of spherical voids in microscopic models. However, the void creation routine is extendable to other shape ratio, requiring extended experimental data on the void shape distributions.

Evaluation of material scatter in composite unit cells

In the previous sections, a framework has been developed to generate stochastic unit cells of resin material and unidirectional composite. Using the experimental measurements of section 2, several sources of scatter and their effect on the mechanical properties are investigated with a metamodel-based Monte-Carlo analysis using the optimization software LS-OPT Table 3.[46]

Computation scheme and parameter investigation

The complexity of characterizing composite materials comes from the difficulty to separate the sources of scatter and investigate them independently on an experimental basis. The present approach allows for an independent

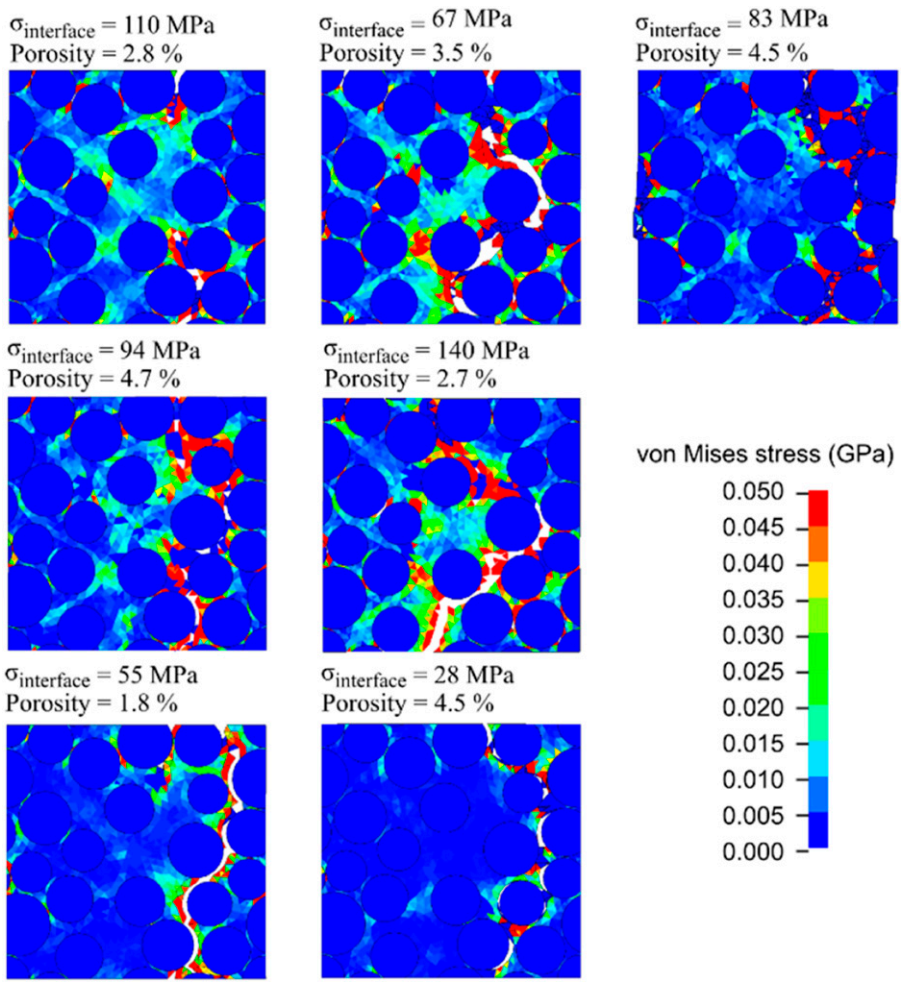

Figure 13. Failure mechanisms under transverse tension for unit cells with stochastic inputs.

consideration of these defects. In a first step, the effect of porosity and pore size on the behaviour of neat resin material is studied. For this, the original deterministic unit cell is attributed randomly distributed material properties and pores (Figure 8 left). In a second step, the same methodology is applied to the unit cells of a unidirectional composite under transverse tension by adding the interface strength as further scatter variable (Figure 8 right). The postprocessing of the results leads to a metamodel quantifying the influence of each source of scatter (listed in Table 3).

Numerical results

Neat resin material. Figure 9 shows the relationship between the degree of porosity, the size of the pores and the mechanical properties of the neat resin material. The elastic properties of the material are negatively impacted by both the porosity and the pore size. A decrease by 10% of the elastic properties is observed at a porosity of 5% and for a pore size of 1.8 mm compared to a non-porous model. A strong influence of the mean pore size on the material strength is predicted by the current modelling approach. At a pore size of 1.8 mm, the strength is only half of the pristine value. This effect is caused by the resulting stress concentration in the vicinity of the voids that causes plastic deformation of the model at a lower global strain state (Figure 10). This plastic deformation increases at higher porosity as the distance between the voids decreases. At the higher pore size, a stress concentration of 1.6 has been observed in the finite-element simulation, compared to 1.2 for lesser pore sizes.

Impregnated fibre cluster. In a first analysis on the microscale, the relationship between the mechanical properties and the porosity and pore size are investigated independently on other factors (Figure 11). The present model depicts a similar detrimental effect of pores on the transversal stiffness and strength as similarly predicted in literature works with geometrical models of the pores for carbon composites.[7–9] In particular, Chu and Jiang numerically predicted a drop of the transverse modulus of

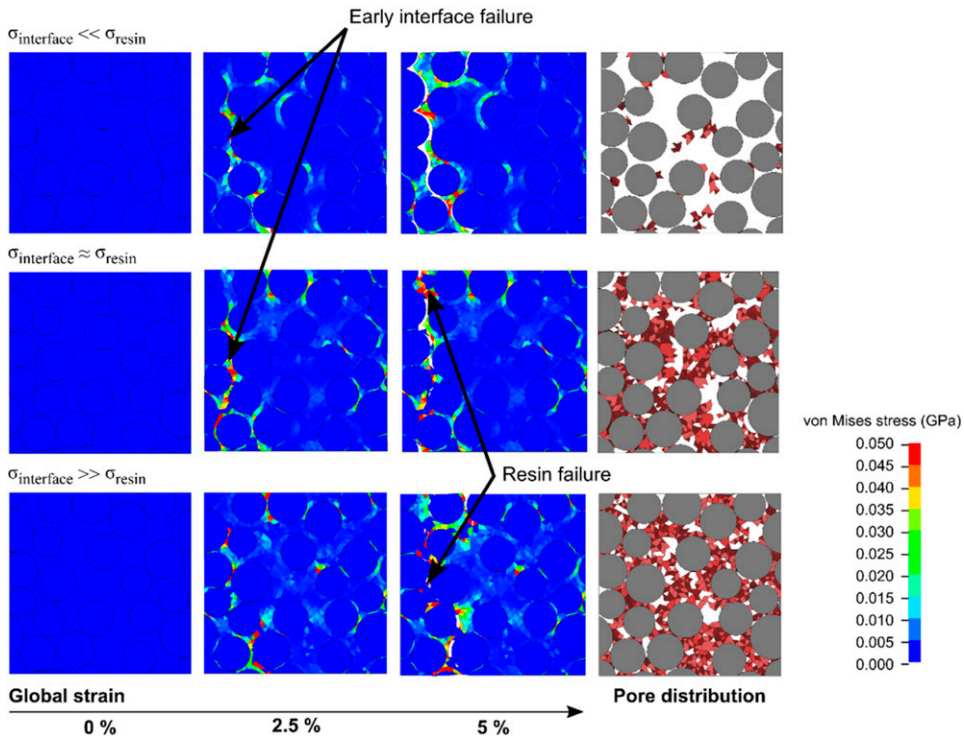

Figure 14. Crack initiation and propagation at different interface strengths and with different porosities.

about 10% at a void content of 4%, which correlates well with the present numerical results.[8,47] He[7] and Liu[12] predicted a strength drop between 15% and 25% at the same void content, which agrees well with the observed 15% drop in this work. With about 90,000 tetrahedron elements compared to the 600,000 used by Chu in Ref. 8, the present approach represents a strong reduction of the computational time assuming the use of similar material models and finite-element solver. The same observation can be made for the modelling approach used by Jiang.[47] It involves 32,000 hexahedron elements for a unit cell size of 24 × 13 × 1 μm³, leading to more than three million elements for a 75 × 75 × 7 μm³ unit cell as investigated in this work. The good correlation between the different modelling techniques overall underlines the potential of the present approach with a simplified representation of the pores. As little information about the actual computational efforts could be found in previous literature works, the efficiency of the present approach can only be estimated based on available data about the mesh size, which is in linear relationship with the critical timestep.

In the second Monte-Carlo analysis, the combined influence of the scatter sources is investigated (Figure 12). Overall, the fibre/resin interface strength represents the major contribution to the material strength for most of the pore configurations investigated. A low adhesive strength, resulting from imperfect manufacturing processes or from incompatible fibre/resin combinations, significantly decreases the transverse strength (Figure 13). The different failure mechanisms due to difference between the neat resin strength and the interface strength are correctly reproduced as depicted in Figure 14. For low interface strengths, cracks are initiated at the intersection between fibres and in the vicinity of pores at low global strain levels. The crack network develops further until a crack front occur in the total cross section of the unit cells. The presence of pores accelerates further the crack propagation. As the interface strength increases, matrix plasticization and failure are observed in the unit cell in addition to interface breakage, consequently increasing the material strength (Figure 14).

Conclusion and outlook

In this work, a methodology based on microscopic numerical simulations was developed in this work to analyse the influence of different scatter sources on the mechanical properties of neat resin and unidirectional composites. Experimental measurements of the porosity, pore size and fibre distribution characteristics were performed and defined the boundary conditions for a Monte-Carlo analysis. Additionally, variations in the interface strength have been added to the study. While the results of the analysis show a strong relationship between the porosity and the neat resin properties, a lower correlation was observed on the microscopic model and only the interface strength appeared to have a major influence on the material strength. The present

representation of pores through a local change of the material properties performs well in comparison to the models with geometrical representations of the pores. In particular, it represents accurately stress concentration in the vicinity of the pores.

Applied on a full multiscale framework, the present approach would allow for the precise quantification of scatter sources and of their effect at every material scale and enable the prediction of the probability of failure on the structural level. Of particular interest is the investigation of uncertainty sources at the mesoscopic and macroscopic levels. On those material scales, scatter sources from the lower scales are adding up, influencing even more the mechanical properties of the material. The current probabilistic approach could guide and support the definition of mechanical testing campaigns or the further development and improvement of manufacturing processes by analysing the most sensitive and relevant parameters for various loading scenarios.

Declaration of conflicting interests

The author(s) declared no potential conflicts of interest with respect to the research, authorship, and/or publication of this article.

Funding

The author(s) disclosed receipt of the following financial support for the research, authorship, and/or publication of this article: This work was supported by the German Federal Ministry of Education and Research within the framework of the ARENA2036 project "Digitaler Fingerabdruck" (grant number 02P18Q602) and managed by the Karlsruhe Institute of Technology.

ORCID iDs

Mathieu Vinot https://orcid.org/0000-0003-3394-5142
Christian Liebold https://orcid.org/0000-0002-6128-2350

References

1. Lukaszewicz D-J. Automotive composite structures for crashworthiness. *Adv Compos Mater Automotive Appl Struct Integrity Crashworthiness* 2013.
2. European Union Aviation Safety Agency. Certification specifications and acceptable means of compliance for large aeroplanes CS-25. *Eur Union Aviation Saf Agency* 2020.
3. Federal Aviation Administration, AC 20-107B - composite aircraft structure. 2009.
4. Llorca J, González C, Molina-Aldareguia J, et al. Multiscale modeling of composites: toward virtual testing ... and beyond. *JOM: J Minerals, Met Mater Soc* 2012.
5. Zhang J, Shields M and TerMaath S. Probabilistic modeling and prediction of out-of-plane unidirectional composite lamina properties. *Mech Adv Mater Struct* 2020; 24.
6. Arregui-Mena JD, Margetts L and Mummery P. Practical application of the stochastic finite element method. *Arch Comput Methods Eng* 2014.
7. He C, Ge J, Cao X, et al. The effects of fiber radius and fiber shape deviations and of matrix void content on the strengths and failure mechanisms of UD composites by computational micromechanics. *Compos Sci Technol* 2022.
8. Chu Y, Sun L, Yang X, et al. Multiscale simulation and theoretical prediction for the elastic properties of unidirectional fiber-reinforced polymer containing random void defects. *Polym Compos* 2021; 42: 2958–2972.
9. Hyde A, He J, Cui X, et al. Effects of microvoids on strength of unidirectional fiber-reinforced composite materials. *Compos Part B: Eng* 2020.
10. Turteltaub S and de Jong G. Multiscale modeling of the effect of sub-ply voids on the failure of composite materials. *Int J Sol Struct* 2019; 165: 63–74.
11. Liu T, Fan W and Wu X. Comparisons of influence of random defects on the impact compressive behavior of three different textile structural composites. *Mater Des* 2019; 181: 23.
12. Liu Z, Lei Y, Zhang X, et al. Effect mechanism and simulation of voids on hygrothermal performances of composites. *Polymers* 2022.
13. Melro A, Camanho P, Pires FA, et al. Micromechanical analysis of polymer composites reinforced by unidirectional fibres: part II - micromechanical analyses. *Int J Sol Struct* 2013; 50: 1906–1915.
14. Swolfs Y, Verpoest I and Gorbatikh L. Issues in strength models for unidirectional fibre-reinforced composites related to Weibull distributions, fibre packings and boundary effects. *Compos Sci Technol* 2015; 114: 42–49.
15. AhmadvashAghbash S, Fazlali B, Mehdikhani M, et al. Finite element analysis of the effect of longitudinal debonding on stress redistributions around fibre breaks in randomly packed fibres. *Compos Sci Technol* 2022.
16. Zheng T, Guo L, Benedictus R, et al. Micromechanics-based multiscale progressive failure simulation of 3D woven composites under compressive loading with minimal material parameters. *Compos Sci Technol* 2022.
17. Tao Z, Guo L, Ding J, et al. An innovative micromechanics-based multiscale damage model of 3D woven composites incorporating probabilistic fiber strength distribution. *Compos Struct* 2022.
18. Mehdikhani M, Petrov N, Straumit I, et al. The effect of voids on matrix cracking in composite laminates as revealed by combined computations at the micro- and meso-scales. *Compos Part A: Appl Sci Manuf* 117: 180–192.
19. Bostanabad R, Liang B, Gao J, et al. Uncertainty quantification in multiscale simulation of woven fiber composites. *Computer Methods Appl Mech Eng* 2018; 338: 506–532.
20. Chiachio M, Chiachio J and Rus G. Reliability in composites–a selective review and survey of current development. *Compos: Part B* 2011; 43: 902–913.

21. DIN Deutsches Institut für Normung e.V., DIN EN ISO 527-2: bestimmung der zugeigenschaften Teil 2: prüfbedingungen für form- und extrusionsmassen. Beuth, Berlin, 1994.
22. Rasband W. Image J - image processing and analysis in java. [Online]. Available: https://imagej.nih.gov/ij/ (Accessed 15 Decembre 2021).
23. Pistori H, Costa ER and Schulze M. *ImageJ docs - Hough circle transform*. University of California, Berkeley Vision Sciences. [Online]. Available: https://imagej.net/plugins/hough-circle-transform (Accessed 15 Decembre 2021).
24. Schuld A. *Simulation des verformungs- und schädigungsverhaltens thermoplastischer faserverbundwerkstoffe mittels parametrischer mehrskaliger werkstoffmodelle*. Bochum: Fakultät für Maschinenbau der Ruhr–Universität Bochum, 2014.
25. Vaughan T and McCarthy C. A combined experimental–numerical approach for generating statistically equivalent fibre distributions for high strength laminated composite materials. *Compos Sci Technol* 2010; 70: 291–297.
26. Koutrouvelis I, Canavos G and Meintanis S. Estimation in the three-parameter inverse Gaussian distribution. *Comput Stat Data Anal* 2004; 8: 1132–1147.
27. Cartié D and Irving P. Effect of resin and fibre properties on impact and compression after impact performance of CFRP. *Compos: Part A* 2001; 33: 483–493.
28. Yoo H, Kim M, Kim B, et al. Impact and shear properties of carbon fabric/poly-dicyclopentadiene composites manufacturedby vacuum-assisted resin transfer molding. *E-Polymers* 2019; 19: 437–443.
29. Warrior N, Turner T, Robitaille F, et al. Effect of resin properties and processing parameters on crash energy absorbing composite structures made by RTM. *Compos: Part A* 2003; 34: 543–550.
30. Pardoen T, Klavzer N, Gayot S, et al. Nanomechanics serving polymer-based composite research. *Comptes Rendus Physiques* 2021; 22: 331–352.
31. Chevalier J. *Micromechanics of an epoxy matrix for fiber reinforced composites : experiments and physics-based modelling*. Louvain: Université Catholique de Louvain, 2022.
32. Hardiman M, Vaughan T and McCarthy C. A review of key developments and pertinent issues in nanoindentation testing of fibre reinforced plastic microstructures. *Compos Struct* 2017; 180: 782–798.
33. Gerlach R, Siviour C, Petrinic N, et al. Experimental characterisation and constitutive modelling of RTM-6 resin under impact loading. *Polymer* 2008; 49(11): 2728–2737.
34. Riaño L, Belec L, Chailan J-F, et al. Effect of interphase region on the elastic behavior of unidirectional glass-fiber/epoxy composites. *Compos Struct* 2018; 198: 109–116.
35. Ren M, Zhang X, Huang C, et al. An integrated macro/micro-scale approach for in situ evaluation of matrix cracking in the polymer matrix of cryogenic composite tanks. *Compos Struct* 2019; 216: 201–212.
36. DIN Deutsches Institut für Normung e.V.. DIN EN ISO 527-1 - kunststoffe - bestimmung der zugeigenschaften - Teil 1: allgemeine grundsätze. Beuth, Berlin, 2012.
37. LIMESS Messtechnik & Software GmbH. LIMESS messtechnik & software GmbH. [Online]. Available: https://www.limess.com/de/ (Accessed 15 Decembre 2021).
38. Sun C and Vaidya R. Prediction of composite properties from a representative volume element. *Compos Sci Technol* 1995; 56: 171–179.
39. Gigliotti L and Pinho S. Enabling faster structural design: efficient multiscale simulation of large composite structures. In: 20th internation conference on composite materials, Copenhagen, Denmark, 19–24 July 2015.
40. Wang W, Dai Y, Zhang C, et al. Micromechanical modeling of fiber-reinforced composites with statistically equivalent random fiber distribution. *Materials* 2016.
41. D´Mello R and Waas A. Influence of unit cell size and fiber packing on the transverse tensile response of fiber reinforced composites. *Materials* 2019.
42. Shah S and Maiarù M. Effect of manufacturing on the transverse response of polymer matrix composites. *Polymers* 2021.
43. Chao Z, Curiel-Sosa J and Bui T. Comparison of periodic and free mesh on the mechanical properties prediction of 3D braided composites. *Compos Struct* 2016; 159: 667–676.
44. Livermore Software Technology (LST), an ANSYS Company. *LS-DYNA keyword user's manual - volume II material models*. California: Livermore Software Technology (LST), 2020.
45. DYNAmore GmbH. *ENVYO User's manual*. Stuttgart, Germany: DYNAmore GmbH, 2021.
46. Livermore Software Technology Corporation. LS-OPT® user's manual: a design optimization and probabilistic analysis tool for the engineering analyst. California, 2020.
47. Jiang H, Ren Y, Liu Z, et al. Microscale finite element analysis for predicting effects of air voids on mechanical properties of single fiber bundle in composites. *J Mater Sci* 2018; 54: 1363–1381.